

**NUMERICAL MODELING OF POROSITY ALTERATION AT THE SUB-SURFACE OF IMPACTS IN SANDSTONE.** N. Güldemeister<sup>1</sup>, K. Wünnemann<sup>1</sup>, E. Buhl<sup>2</sup>, T. Kenkmann<sup>2</sup>, N. Durr<sup>3</sup> and S. Hiermaier<sup>3</sup>, <sup>1</sup>Museum für Naturkunde, Invalidenstrasse 43, 10115 Berlin, Germany (nicole.gueldemeister@mf-n-berlin.de), <sup>2</sup>Institut für Geowissenschaften, Albert-Ludwigs-Universität Freiburg, Germany, <sup>3</sup>Fraunhofer Institute for High-Speed Dynamics, Ernst-Mach Institute (EMI), Freiburg, Germany

**Introduction:** Porosity plays an important role in impact crater formation and shock wave propagation. In previous studies the effect of an initially present porosity that is crushed out during shock wave compression on crater efficiency [1,2,3], shock pressure and decay, shock-induced heating and melting [4,5], and ejection of material [6] has been investigated. However, a quantitative understanding of the increase in porosity in rocks due to unloading from shock pressures and tensile stresses is lacking so far. The opening of pore space as a result of the rarefaction wave following shock compression may be related to the observed geophysical anomalies at impact craters. In the framework of the “MEMIN” (Multidisciplinary Experimental and Modeling Impact crater research Network) project, the effects of hypervelocity impact shock compression and subsequent release in porous sandstone are investigated. Iron spherules (2.5-12 mm in diameter) were shot at velocities between 2-8 km/s on dry and water-saturated sandstone blocks producing craters 5-29 cm in diameter [e.g. 7,8]. Sampling of the crater subsurface enables measuring of the change in petrophysical properties and quantifying target deformation including fracturing and compaction. Microanalyses of thin sections provide pore space distributions as a function of distance to the crater floor [9]. The laboratory impact experiments were accompanied by numerical modeling in order to quantify processes beyond the observational capabilities and to validate newly developed numerical methods.

**Observations:** The detailed analyses of samples from the crater subsurface are presented in the company paper [9]. Here we refer only to the impact experiment with a 2.5 mm steel sphere impacting at 4.8 km/s a 20 cm cubed dry sandstone with an initial porosity of ~22%. The resulting crater has a diameter of 5.76 cm and a depth of 1.1 cm. Fig. 1 shows the change in porosity up to 10 mm below the crater floor. Composite backscatter electron micrographs give a qualitative impression of the porosity alteration. Image analysis software was used to determine porosity as a function of depth [9]. Near the crater floor porosity exceeds the initial porosity, which is most likely caused by the formation of tensile cracks parallel to the crater floor as a result of shock wave release. With increasing distance from the crater floor porosity decreases due to shock wave compression. Apparently, at a distance of approximately 6 mm the amplitude of the shock wave

has dropped below the crushing strength of pores and no pore space is crushed out.

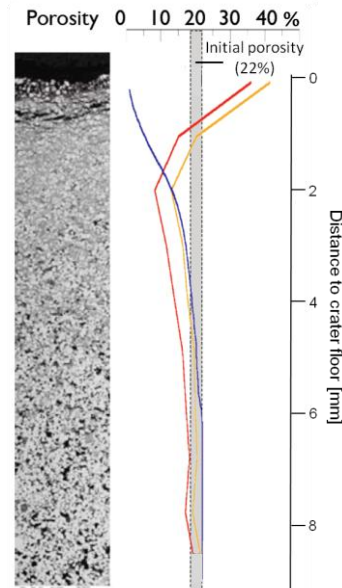


Fig. 1: Porosity as function of depth along a vertical profile underneath the crater floor. Left hand side shows backscatter electron micrographs, right hand side depicts the measured maximum (yellow) and minimum porosity (red). The blue line shows the porosity determined by numerical modeling.

**Numerical modeling:** To simulate crater formation and shock wave propagation in the experiment described above we use the multi-material, multi-rheology hydrocode iSALE [10,11, and references in there] coupled with ANEOS [12] and the  $\epsilon$ - $\alpha$  porosity compaction model [10]. In our model porosity is considered as a state variable, the distension  $\alpha$ , that decreases if negative volumetric strain (compression) occurs. Note, the porosity model only accounts for compaction and does not consider re-opening of cracks due to tension. The model is capable to reproduce crater formation (not shown here) and the crushing of pore space due to shock wave propagation below the crater floor fairly well. Fig. 1 shows a comparison between the observed and modeled crushing curves (porosity as a function of distance). The zone directly underneath the crater floor where porosity is increased due to tension cannot be simulated as an appropriate physical model to describe opening of pore space due to tensile bulking is lacking so far. To further investigate the shock unloading process we approximate the conditions by a

planar impact model where a flyer plate (“projectile”) with a given velocity impacts on a buffer plate (“target”) generating a well-defined planar shock wave. The reflection of the shock wave at the free surface of the flyer plate releases a rarefaction wave unloading the material from shock pressure. We used dry materials with an initial porosity of 20%. The simulation shows that the material in the direct proximity to the free-surface experiences negative pressures during the passage of the rarefaction wave (Fig. 2, magnification frame). From the physical point of view these negative pressures are the result of high tension which may be as large as the maximum compressional stress. However, negative pressures and high tensile stresses are unphysical because the tensile stresses exceed the tensile strength of the target. To eliminate such unphysical conditions we add porosity to the computational cells (increase the state variable  $\alpha$ ) until the pressure converges to zero. In other words, volumetric expansion is compensated by introducing pore space. Note, mass and energy are conserved in the described procedure.

**Preliminary results:** Fig. 2 shows profiles of pressure (left) and porosity (right) at different points in time during the simulation. As the shock wave (blue) propagates up into the buffer plate and down into the target pore space is completely crushed out. The rarefaction wave re-introduces pore space where negative pressures occur. The final porosity reaches values of the initial porosity. The extent of the area where pore space is added and the amount of generated porosity depend on the amplitude of the shock wave. In a next step the new model to describe the increase of porosity by shock unloading will be tested in simulations of the MEMIN experiments and compared to the observed porosity profiles described above.

**Discussion:** Numerical models show in general a

good agreement with the compaction of porosity underneath the crater floor neglecting the region near to the impact surface. The preliminary results from models of planar impact show that the new model is capable to describe an increase of porosity as a response to unloading of shock. However in the simulation we only increase the porosity up to the initial porosity which is less than the porosity that was reached in the experiment (up to two times the initial porosity). This may be explained by the opening of tensile flaws that occur beneath the surface which raise the experimentally determined porosity to such high porosities. The used  $\epsilon$ - $\alpha$  porosity model does not resolve single open pore space, fractures or flaws. In the given approach pore space is opened by adjusting the porosity value in accordance with the thermodynamic conditions. Thus, localized fractures as observed in the laboratory experiments cannot be modeled by the proposed method that accounts only for the bulk behavior of material after shock release. In the future, we plan to combine a tensile failure model with the thermodynamically driven expansion of matter after shock release. We will also investigate the influence of decompression on porosity at the subsurface in water-saturated materials.

**Acknowledgment:** This work was funded by DFG grant WU 355/6-1.

**References:** [1] Love S. G. et al. (1993) *Icarus*, 105, 216-224. [2] Wünnemann K. et. al. (2006) *Icarus*, 180, 514-527. [3] Wünnemann et al. (2010), *HVIS*. [4] Wünnemann et al. (2008) *EPSL*, 269, 529-538. [5] Kraus et al. (2010) *EPSL*, 289, 162-170. [6] Collins G.S. et al. (2007), 38<sup>th</sup> LPSC #1620. [7] Kenkmann T. et al. (2011) *MAPS* 46 875-889. [8] Schäfer F. et al. (2006) ESA SP-612. [9] Buhl. et al. (2011) 43<sup>th</sup> LPSC, this volume. [10] Wünnemann K. et. al. (2006) *Icarus*, 180, 514-527. [11] Ivanov, B. A., et al. (1997), *Int. J. Imp. Eng.* 20, 411-430. [12] Thompson S. L and Lauson H. S. (1972), SC-RR-71 0714, 119pp.

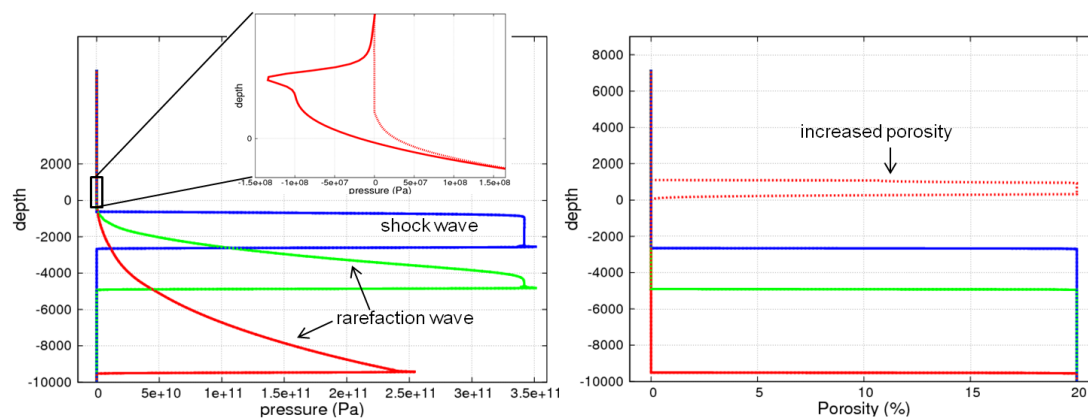


Fig. 2: Pressure (left) and porosity (right) profiles at different points in time (blue, green, red). The pressure profile shows the shock wave and the followed rarefaction waves. The magnification represents the area with negative pressures. The dashed line shows the pressure after adjusting the porosity. The previously negative pressures now converge to zero which results in an increase of porosity as seen in the porosity profile (dashed line). The solid lines represent the state of pressure and porosity before the porosity is increased. After the passage of the shock wave the porosity is crushed.